Biogeosciences
Discussions

Open Access

EGU

# Gas chromatography vs. quantum cascade laser-based N$_2$O flux measurements using a novel chamber design

Christian Brümmer[1,*], Bjarne Lyshede[1], Dirk Lempio[1], Jean-Pierre Delorme[1], Jeremy J. Smith[1], Roland Fuß[1], Antje M. Moffat[1], Miriam Hurkuck[1], Andreas Ibrom[2], Per Ambus[3], Heinz Flessa[1], Werner L. Kutsch[1,4]

[1]Thünen Institute of Climate-Smart Agriculture, Braunschweig, Germany
[2]Department of Environmental Engineering, Technical University of Denmark, Lyngby, Denmark
[3]Department of Geosciences and Natural Resource Management, University of Copenhagen, Denmark
[4]Integrated Carbon Observation System (ICOS), Head office, Helsinki, Finland

*Correspondence to*: Christian Brümmer (christian.bruemmer@thuenen.de)

**Abstract.** Recent advances in laser spectrometry offer new opportunities to investigate soil-atmosphere exchange of nitrous oxide. During two field campaigns conducted at a grassland site and a willow field, we tested the performance of a quantum cascade laser (QCL) connected to a newly developed automated chamber system against a conventional gas chromatography (GC) approach using the same chambers plus an automated gas sampling unit with septum capped vials and subsequent laboratory GC analysis. Through its high precision and time resolution, data of the QCL system were used for quantifying the commonly observed non-linearity in concentration changes during chamber deployment, making the calculation of exchange fluxes more accurate by the application of exponential models. As expected, the curvature in the concentration increase was higher during long (60 min) chamber closure times and under high flux conditions ($F_{N2O}$>150 μg N m$^{-2}$ h$^{-1}$) than those that were found when chambers were closed for only 10 min and/or fluxes were in a typical range of 2 to 50 μg N m$^{-2}$ h$^{-1}$. Extremely low standard errors of fluxes, i.e. ~0.1 % of the flux value, were observed regardless of linear or exponential flux calculation when using QCL data. Thus, we recommend reducing chamber closure times to a maximum of 10 min when high-frequency measurements are available to keep soil disturbance low and conditions around the chamber plot as natural as possible. If instrumentation with high-frequency resolution is available, sampling times from 1 to 5 s proved to be sufficient for robust flux determination assuring standard errors of N$_2$O fluxes still being on a relatively low level. Despite low signal to noise ratios, GC was still found to be a useful method to determine soil-atmosphere exchange of N$_2$O at longer time scales, i.e. seasons to years, e.g., when the main focus of the study is to investigate site budgets. Intriguingly, the consistency between GC and QCL-based campaign averages was better under low than under high N$_2$O efflux conditions, although single flux values were highly scattered during the low efflux campaign. Furthermore, the QCL technology provides a useful tool to accurately investigate the highly debated topic of diurnal courses of N$_2$O fluxes and its controlling factors. Our new chamber design reduces the disturbance of the soil and complies with high quality requirements of long-term observation studies and research infrastructures.

## 1 Introduction

Accurate determination of ambient nitrous oxide ($N_2O$) concentrations and the associated exchange between soil and atmosphere has been in the focus of environmental research for several years. Nitrous oxide is of high relevance for the Earth's greenhouse gas budget due to its long residence time in the troposphere and its relatively large energy absorption capacity per molecule, resulting in a cumulative radiative forcing almost 300 times higher than the same mass unit of carbon dioxide over a 100-year period when climate-carbon feedbacks are included (IPCC, 2013). It is predominantly emitted as a byproduct of nitrification and an intermediate product of denitrification and nitrifier denitrification, which are key microbiological processes in the soil nitrogen (N) cycle (Firestone and Davidson, 1989; Wrage et al., 2001; Thomson et al., 2012; Butterbach-Bahl et al., 2013). Main $N_2O$ sources are agricultural activities in the form of N fertilization. In smaller quantities, $N_2O$ is also produced through biomass burning, degassing of irrigation water, and industrial processes (Seinfeld and Pandis, 2006). On the other hand, some field studies report that soils can also consume $N_2O$, albeit the strength of this sink has not yet been thoroughly evaluated (Donoso et al., 1993; IPCC 2007; Chapuis-Lardy et al., 2007).

Precise measurements of $N_2O$ – particularly at the field scale – are therefore essential for specific applications in ecosystem research such as the study of N cycling, fertilization effects, and for the compilation of full greenhouse gas budgets. The most common method to measure soil-atmosphere exchange of $N_2O$ is the operation of static chambers (Hutchinson and Mosier, 1981; Schiller and Hastie, 1996). The $N_2O$ flux is calculated from the concentration increase (or decrease) over time in a gas-tight chamber, which is usually attached to a collar that is permanently inserted into the soil. A number of approaches have emerged over the last years where the air sample is either manually collected using a syringe through a septum and/or directly inserted into sample vials (e.g., Castaldi et al., 2010; Jassal et al., 2008, 2011; Livesley et al., 2011; Lohila et al., 2010; Parkin and Venterea, 2010 and references therein) with subsequent analysis on gas chromatography (GC) systems using $^{63}Ni$ electron capture detectors for $N_2O$ detection. Different chamber designs and air sampling procedures exist, either with manual, semi-automated, i.e. automatic sampling but manual transport of air samples in syringes or vials to the GC (this study), or fully automated gas collection, where the air samples are directly pumped (or sucked) via carrier gas to a temperature-stable housing equipped with a GC in the field (e.g., Brümmer et al., 2008; Butterbach-Bahl et al., 1997; Dannenmann et al., 2006; Flessa et al., 2002; Papen and Butterbach-Bahl, 1999; Rosenkranz et al., 2006).

In the last decade, substantial progress has been made in the development of fast-response technologies for analyzing a variety of N and carbon (C) trace gases. These are tunable diode laser absorption spectrometers (TDLAS), quantum cascade lasers (QCL) and devices originating from individual applications such as Fourier transform infrared (FTIR) spectrometers or custom-made converters coupled to chemiluminescence detectors (CLD). These robust, fast and precise analyzers are essential for long-term monitoring of biosphere-atmosphere exchange and have even allowed first eddy covariance (EC) measurements of field-scale $N_2O$, methane ($CH_4$) (e.g., Rinne et al., 2005; Denmead et al., 2010; Kroon et al., 2010; Neftel et al., 2010; Tuzson et al., 2010; Jones et al., 2011; Merbold et al., 2014), and reactive N fluxes (Horii et al., 2004; Ammann et al., 2012; Brümmer et al., 2013). Continuous observations of trace gas exchange over time scales from hours to decades

enable researchers to evaluate diurnal, seasonal and interannual variability and trends as well as the elucidation of climatic and management controls on gas exchange patterns (e.g., Baldocchi et al., 2001; Brümmer et al., 2012; Kutsch et al., 2010). With regard to chamber measurements, it is expected that the precision and time resolution of the above-mentioned technologies may considerably reduce the chamber closure duration for single flux measurement events, thereby minimizing

5    plot disturbance and allowing for a significant increase in repeated measurements leading to more robust databases, which are required for reliable greenhouse gas budgets. Although the EC methodology provides near-continuous time series of greenhouse gas concentrations and exchange, chamber measurements will certainly still be required in the future as prerequisites for EC measurements are sometimes not fulfilled (for example through insufficient turbulent mixing, complex terrain, inhomogeneous fetch) and small-scale spatial variability or emissions from replicated field plot experiments can only

10   be determined by chamber measurements.

The comparability, applicability and uncertainty associated with the respective approach are currently debated in the ecosystem research community, e.g. when comparing fluxes from GC/vial systems with those from more recent continuous setups such as QCL systems. In this context, the flux determination method was found to be an important factor (e.g., Kroon et al., 2008; Forbrich et al., 2010). Fluxes are often calculated using a linear regression of the change in headspace

15   concentration over time and are scaled to the collar area, including a temperature and pressure correction (e.g. Savage et al., 2014). However, several other studies demonstrate the need for non-linear models for soil-atmosphere trace gas flux estimation (Hutchinson and Mosier, 1981; Livingston et al., 2006; Kutzbach et al., 2007; Kroon et al., 2008; Pedersen et al., 2010; Pihlatie et al., 2013). It has been argued that molecular diffusion theory states that chamber effects lead to declining gradients in the relationship between concentration and time and that slight chamber leakages create the same effect

20   (Hutchinson and Mosier, 1981; Livingston et al., 2006; Pedersen et al., 2010). Nevertheless, linear concentration data often predominates (e.g. Forbrich et al., 2010), which may not necessarily be in conflict with the theory as non-linearity is sometimes not visible in data series with only a limited number of samples (mostly due to noisy concentration measurements or effects of small chambers; Pedersen et al., 2010).

To further investigate effects of flux estimation methods on the one hand and the use of different gas analyzer types on the

25   other hand, our study comprises $N_2O$ chamber flux measurements from two campaigns conducted under different environmental conditions with the aim to (1) present a novel chamber design used in both an automated vial air-sampling setup followed by gas chromatography analysis in the laboratory and in combination with a directly connected QCL system, (2) test different flux calculation methods, i.e. conventional linear regression models vs. a slightly modified HMR procedure (Hutchinson-Mosier Regression, *cf.* Pedersen et al., 2010), including different chamber closure durations, and sampling

30   frequencies to find an optimal setup particularly for the QCL system, and to (3) compare single and mean fluxes of the field campaigns to help recommending an appropriate setup for common field applications.

## 2 Methods

### 2.1 Chamber design

Nitrous oxide measurements were carried out using a newly developed semi-automatic chamber system (Figure 1). It consisted of aluminum guiding racks (length 2121 mm, width 936 mm, height 3033 mm) with aluminum soil collars (length

5   750 mm, width 750 mm, height 160 mm, inserted 0.10 m into the soil), and opaque PVC chambers (color white, interior dimensions: length 777 mm, width 777 mm, height 565 mm) (Ps-plastic, Eching, Germany). The chambers have a headspace volume of 0.33 $m^3$ and covered a surface area of 0.56 $m^2$. Depending on vegetation height, extension modules (interior dimensions: length 730 mm, width 730 mm, height 360 mm) can be connected to the chambers (total headspace volume was then 0.54 $m^3$) if needed over taller vegetation, but were not used in this study. EPDM-gaskets (20 mm x 15 mm) were

10   attached to the bottom of each chamber in an aluminum u-channel to ensure gas tight closure when chambers were operating. Up to three chambers can be combined to one system (Figure 1B) with a joint control unit and autosampler or analyzer. Two custom made temperature probes (Pt100) were installed inside and outside of each chamber to measure ambient air temperatures. Chambers were ventilated during measurements using an axial fan. The air was sampled from the top centre of the lids. Chamber operation was controlled by a logic module (Millenium 3, Crouzet, Hilden, Germany). An autosampler

15   consisting of a membrane pump (operated at 0.8 L $min^{-1}$, NMP 830 KNDC, KNF Neuberger, Freiburg, Germany), an absorber to avoid water condensation within tubes (3.2 mm ID, 6.4 mm OD) (BEV-A-Line, ProLiquid GmbH, Überlingen, Germany) and valves as well as an exchangeable rack for 162 headspace vials (20 mL, WICOM WIC 43200, Maienfeld, Germany) were connected to the chamber system. Chambers were lifted and moved down by a 24 V (DC) motor winch and were directed to the soil collar by the aluminum rack. After measurement events, the chamber was lifted to 1.18 m above

20   ground and dragged backwards in a 45° angle to keep the soil and vegetation inside the soil collar under as natural conditions as possible (e.g. prevention of shading and undisturbed throughfall). To avoid pressure changes when setting the chamber on the collar, the chamber had a 1.5 m pressure compensation tube leading from the inside through the side wall of the chamber to the outside.

### 2.2 Campaigns and measurement setup

25   Two field campaigns were conducted in fall 2012 in Braunschweig, Germany, and in spring 2013, at Risø Campus, Technical University of Denmark, using both GC and QCL chamber setups (see Table 1 for additional information). The chamber architecture was identical during the two campaigns. Sites and time periods were selected with the aim to compare chamber system performance under high and low flux conditions. Due to low temperatures and no fertilizer applied, we expected a low exchange regime during the Braunschweig campaign, whereas higher fluxes were expected at Risø (higher

30   temperatures and a substantial amount of fertilizer applied).
During parallel operation of GC and QCL, chambers were closed for 60 minutes at both sites to measure the concentration increase. When only QCL measurements were conducted, i.e. at Risø at DOY <105.5 and DOY >108.5, chambers were

closed for only 10 minutes. For the GC setup, four air samples were taken at 0, 20, 40, and 60 minutes after chamber closure to calculate one flux rate. Air samples (20 mL) were pumped through the tubing system using a membrane pump (3.2 L min$^{-1}$, NMP 830 KNDC, KNF Neuberger, Freiburg, Germany) and were injected into septum-capped vials. Two cannulas were automatically inserted through the septum, one cannula acting as sample air inlet until overpressure was established,

5 and the other cannula acting as outlet for cycling the air back to the chamber. Air samples were stored in the exchangeable rack of the autosampler unit and were analyzed in the GC-lab of the Thünen Institute using a GC-2014 (Shimadzu, Duisburg, Germany; modified according to Loftfield et al., 1997) with an electron capture detector for $N_2O$ analysis. Performance of the GC-system was checked weekly by conducting ten consecutive measurements of a standard gas with ambient $N_2O$ concentration (320 ppb). Samples were only analyzed if the coefficient of variation of peak areas during this test was below

10 3 %.

Parallel to the autosampler setup for GC analysis, we operated our chamber system directly connected to a QCL (continuous-wave quantum cascade laser absorption spectrometer, model mini-QCLAS, Aerodyne Research Inc., Billerica, Massachusetts, USA; see Nelson et al. (2004) for principle of operation) in a thermo-controlled housing. Briefly, the laser is thermoelectrically cooled (Thermocube) to 25 °C, uses a 76-m path length, 0.5 L volume and multiple pass absorption cell

15 for sampling, and operates at 40 Torr. It provides a measurement precision of 0.04 ppb ($1\sigma$) within an averaging interval of one second. Calibration is performed by continuously aligning the $N_2O$ absorption peak of the sampled air to the standard of the HITRAN database (Rothman et al., 2009). A dry vacuum scroll pump (BOC Edwards XDS10, Sussex, UK) maintained a steady flow rate of 1.0 L min$^{-1}$. After passing the QCL cell, the sample air was cycled back to the respective chamber to avoid underpressure conditions and unintentional sucking of soil air into chambers. Data was stored on the QCL's internal

20 hard drive at a frequency of 10 Hz.

## 2.3 Flux calculation

GC-based $N_2O$ fluxes using linear, robust linear (Huber, 1981), and modified Hutchinson-Mosier regression (HMR; *cf.* Pedersen et al., 2010) were calculated as described in Leiber-Sauheitl et al. (2014) after converting molar concentrations into mass concentrations using temperature but no pressure correction. Briefly, robust linear regression was used as default when

25 four data points were available. Non-linear flux estimation with the HMR method (R Core Team, 2012; HMR package version 0.3.1) was performed when all of the following criteria were met, i.e. (1) the HMR function could be fitted, (2) Akaike information criterion (AIC; Burnham and Anderson, 2004) was lower for HMR fit than for linear fit, (3) *p* value of flux calculated using HMR was lower than that from robust linear fit, and (4) the HMR flux was less than four times larger than the robust linear flux.

30 QCL-based fluxes were estimated using two different methods. We applied the non-linear HMR model with a slightly modified parameterization (Equation 1 this study; *cf.* Moffat, 2012) to the 60-min dataset of a full chamber cycle (10-min cycle in Risø at DOY <105.5 and DOY >108.5) and compared these fluxes with those resulting from an application of linear regression when only the first three minutes of data after chamber closure were used (*cf.* Section 3.2).

To investigate the frequently observed non-linearity in chamber field data, we computed a quantitative parameter $\kappa$ describing the curvature in $N_2O$ concentration increase (or decrease) over time (60-min and 10-min QCL data only). Based on the assumption of exponential gas concentration changes in the chamber (*cf.* Nakano et al., 2004) using

$$c(t) = c_{max}\left(1 - \exp\left(\frac{-k}{c_{max}}t\right)\right) + c_0 \tag{1}$$

with *c(t)* being the $N_2O$ concentration in the chamber at a certain point in time, $c_{max}$ the maximum possible concentration, $c_0$ the measured concentration at *t*=0, and *k* the initial flux $F_0$ divided by the effective chamber height *h*, we estimated the $N_2O$ soil-atmosphere flux as the first derivative of Equation (1) evaluated at *t*=0, i.e.

$$c'(t)|_{t=0} = k \tag{2}$$

and the curvature parameter $\kappa$ as the second derivative of Equation (1) evaluated at *t*=0, i.e.

$$c''(t)|_{t=0} = -\frac{k^2}{c_{max}} = \kappa. \tag{3}$$

Negative values of $\kappa$ correspond to concave curvature indicating a plateauing, i.e. saturating concentration increase over time.

## 3 Results and discussion

### 3.1 Non-linear concentration increase and curvature determination

Significantly different patterns in chamber $N_2O$ concentration changes during the Braunschweig and Risø campaigns were observed (Figure 2). While increases in the order of 10 to 20 ppb per hour (one chamber cycle) were found for the grassland site in Braunschweig, steep concentration increases measured on the harvested willow field at Risø were almost exclusively higher than 100 ppb per hour and reached maximum rates of over 650 ppb per hour in the period from DOY 105.5 to DOY 108.5. For the low exchange regime in Braunschweig, GC-based data points were highly scattered and rarely showed a clear increasing (or decreasing) tendency making flux calculations difficult. For the high exchange regime at Risø, GC-based concentration data were mostly showing well-defined increases and were similar to those obtained by the QCL system (*cf.* Section 3.3). The latter showed a precise and robust performance with clear base line levels and obvious chamber cycles during both campaigns. None of the QCL-based measurements revealed concentration decreases, i.e. negative fluxes ($N_2O$ uptake) while chambers were closed.

The high time resolution of QCL data allowed for a closer look at the increase characteristics and showed that only in a very few cases $c'(t)$ was strictly constant when taking the full 60-min cycle into account. This was expected as the rate of transport of a diffusing trace gas into the chamber headspace necessarily declines throughout deployment because any increase in the headspace concentration results in a corresponding decline in the vertical concentration gradient driving that

5      transport (Rolston, 1986; Hutchinson et al., 2000; Livingston et al., 2006). Results of the investigation on quantifying the curvature in $c(t)$, expressed as $\kappa$, are given in Figure 3.

Extremely low negative $\kappa$ values between $-10^{-4}$ and $-10^{0}$ – indicating quasi linearity in $\partial c/\partial t$ – were almost exclusively found under low flux conditions, whereas fluxes >100 µg N m$^{-2}$ h$^{-1}$ were only observed when $\kappa$ was $< -10^{1}$ (Figure 3A). This means that at higher fluxes the curvature in $c(t)$ is concave suggesting concentrations that tend to plateau over time with

10     the saturation effect becoming larger at higher flux rates. Near zero fluxes, however, corresponding to $\kappa$ values around zero, indicate no considerable changes in N$_2$O concentrations, thus, hardly any alteration of the vertical concentration gradient over time. Furthermore, closure time was found to have an impact on the magnitude of $\kappa$ (Figure 3B). Longer chamber deployment led to higher curvature in $c(t)$, which was expected as concentration gradients decline over time when a considerable flux is measured (*cf.* Hutchinson and Mosier, 1981; Livingston et al., 2006; Pedersen et al., 2010).

15     Our results imply that at low flux rates and/or short chamber closure, the slight non-linearity in concentration change when calculating fluxes is of minor importance and the application of linear models is acceptable, particularly with regard to other commonly observed errors such as those originating from soil disturbance, chamber placement (Christiansen et al., 2011), temperature, pressure and humidity perturbations, etc. (Parkin and Venterea, 2010). At higher fluxes, however, significant curvature in $c(t)$ expressed by large negative $\kappa$ values will most likely lead to a substantial underestimation of fluxes when

20     using linear regression instead of applying an exponential model for flux calculation (*cf.* Matthias et al., 1978; Jury et al., 1982; Anthony et al., 1995; Kroon et al., 2008; Section 3.2). In principle, several other reasons making flux determination with linear or exponential models problematic, may technically be found. These are exponentially increasing N$_2$O concentrations after chamber closure due to possible dispersion effects leading to biased analyzer readings, placement of the sample tube inlet at the top of the chamber lid leading to an establishment of a temporary concentration gradient in a weakly

25     mixed chamber atmosphere or an insufficient dimension of the pressure compensation tube leading to a push back of air into the uppermost soil layer in the moment when the chamber is set onto the lid. However, none of these were observed during our campaigns, thereby indicating a robust setup and chamber design for reliable N$_2$O flux calculations.

We also investigated the possible effect of ambient wind speed and direction on concentration build up characteristics (Figure 3C and 3D, respectively) as differences between the turbulence regime outside the chamber and inside chamber

30     conditions vary under changing wind speed. Theoretically, soil pores might be more ventilated and the coupling of the flux under ambient conditions to the atmosphere is much closer. Consequently, the establishment of a steady state flux may be more postponed under higher wind speed. Such time delay caused by slow filling up of the previously ventilated pore space in parallel to the diffusion into the chamber might in principle explain exponentially increasing concentrations. However, $\kappa$

values (Figure 3C and D) and fluxes (not shown) were independent of both wind speed and direction, which is a further indicator that the chosen chamber design and setup can be used over a wide range of environmental conditions and neither seem to affect concentration build up characteristics nor resulting flux magnitudes.

## 3.2 3-min vs. 60-min closure time in QCL measurements

5    Reviewing past decades of field chamber measurements for studying soil-atmosphere exchange of $N_2O$, several challenges and shortcomings emerged such as limited number of replicates or disturbance of the soil micro-environment due to chamber coverage and soil collar insertion (e.g., Hutchinson and Mosier, 1981; Parkin and Venterea, 2010). One way of getting a higher temporal resolution, thereby a higher number of replicates and keeping soil disturbance as low as possible is to reduce the chamber closure period, which also is expected to decrease deviation from linearity in concentration increase. With the

10    QCL's high time resolution – in this study operated at the analyzer's maximum frequency of 10 Hz – we compared $N_2O$ flux estimates based on 60-min (DOY 105.5 to DOY 108.5) and 10-min (DOY <105.5 and DOY >108.5) closure periods calculated by the modified HMR approach with those flux estimates that are based on the first three minutes of concentration data only and were calculated by linear regression. The Risø dataset was used for this comparison, because both high and low fluxes were observed.

15    Flux estimates of the two approaches matched reasonably well; significant differences were only observed at very high rates (Figure 4A and 4B). 85 % of the variance in $N_2O$ fluxes from 3-min closure could be explained by fluxes from 60-min and 10-min closure (Figure 4B). The relatively high slope of 1.80 was mainly caused by three exceptionally high fluxes where the 60-min method considerably overestimated values of the 3-min method, which could have been caused by disturbances during the 60-min chamber deployment due to soil macrofauna. Recent work e.g. by Kroon et al. (2008) and Forbrich et al.

20    (2010) demonstrated that emission estimates from closed chamber measurements were significantly underestimated when using linear regression methods instead of the slope of an exponential function at the beginning of chamber closure. However, their linear regression models were applied to longer periods, i.e. to 10-min periods by Kroon et al. (2008) also using an Aerodyne QCL spectrometer and to 25-min periods by Forbrich et al. (2010) using a GC setup. Kroon et al. (2008) also showed that linear estimates differed by up to 60 % compared to those from exponential methods with a systematic error due to linear regression being in the same order as the estimated uncertainty due to temporal variation. In our study, standard

25    errors of $N_2O$ fluxes from both 3-min and 60-min closure were extremely low, i.e. in the order of 0.1 % of the fluxes (Figure 4C) with median values of 0.17 and 0.06 µg N m$^{-2}$ h$^{-1}$ and arithmetic means of 0.21 and 0.20 µg N m$^{-2}$ h$^{-1}$ for the 3 and 60-min closure flux estimates, respectively. This implies that limiting the chamber closure period to 3 minutes benefits in two ways. On the one hand, the soil column of interest is less disturbed by shorter coverage and/or the number of replicates can

30    be significantly increased. As these measurements are automated, no further manual work is required. On the other hand, standard errors of fluxes remain extremely low. However, it is recommended to extend the chamber closure period to a minimum of five minutes as slightly delayed concentration increases under low flux regimes (*cf.* Section 3.1) may occur and

would lead to an underestimation of 3-min linear fluxes. We therefore recommend skipping the first 2 minutes of data to guarantee undisturbed conditions that might have been caused in the moment when the chamber is set on the soil collar.

For better comparison with other studies, we also compared HMR-based fluxes with robust linearly calculated fluxes from our GC measurements when the full 60-min cycle was taken into account. A linear regression analysis (data not shown)

5    resulted in a slope of 0.97 and an $R^2$ value of 0.86 under the high flux regime in Risø with the data set of robust linearly calculated fluxes being the independent variable. The mean campaign flux value from HMR-based calculations was 22 % higher than the average campaign value of the robust linear method. The difference between the two methods was even higher under the low flux regime in Braunschweig. Slope and $R^2$ value of a linear regression analysis were 1.82 and 0.42, respectively. Despite the high slope value, the mean campaign value of the robust linear method only reached 51 % of the

10   value obtained from the HMR method.

Furthermore, standard errors were found to depend on QCL sampling frequency (Figure 5). We simulated different sampling times ranging from one tenth of a second to approx. one minute, by excluding the respective intervals from the original 10-Hz dataset. Results showed a clear tendency towards higher standard errors, when fewer data points were included. Arithmetic means of standard errors increased steadily from 0.21 µg N m$^{-2}$ h$^{-1}$ at 10 Hz to 3.36 µg N m$^{-2}$ h$^{-1}$ at 0.03 Hz and

15   from 0.20 µg N m$^{-2}$ h$^{-1}$ at 10 Hz to 2.93 µg N m$^{-2}$ h$^{-1}$ at 0.03 Hz for the 3-min and 60-min method, respectively. These results suggest that – in case no high-frequency measurement devices are available or data storage capacity is limited – sampling times between 1 and 5 seconds are sufficient to keep standard errors of $N_2O$ fluxes on a much lower level than those obtained from GC measurements (*cf*. Section 3.3).

### 3.3 GC vs. QCL-based fluxes under low and high exchange regimes

20   Time series of $N_2O$ fluxes and their associated standard errors using both the GC and the 3-min QCL linear regression method during the Braunschweig and Risø campaigns are given in Figure 6. QCL fluxes in Braunschweig were on a constantly low level ranging between 2 and 16 µg N m$^{-2}$ h$^{-1}$, whereas GC-based fluxes at the same site were scattered between −13 and 39 µg N m$^{-2}$ h$^{-1}$. Less than 1 % of the variance in QCL fluxes could be explained by GC fluxes (Figure 7). While standard errors of the QCL method were always below 0.6 µg N m$^{-2}$ h$^{-1}$, values of the GC method were distributed

25   between 0.5 and 22.0 µg N m$^{-2}$ h$^{-1}$. Although higher variability and higher standard errors in GC-based fluxes were evident, mean $N_2O$ flux rates of the entire observation period were almost identical when comparing the two analyzer types. 6.42 ± 5.98 µg N m$^{-2}$ h$^{-1}$ and 7.77 ± 0.13 µg N m$^{-2}$ h$^{-1}$ were found for the GC and the QCL method, respectively.

Under the high exchange regime at Risø, $N_2O$ fluxes of the two analyzer types matched considerably better (Figure 6D). Although the willow field was already fertilized on DOY 99, $N_2O$ fluxes did not start to increase until DOY 105 when a

30   sharp rise in air temperature was observed. GC-based fluxes were lower than QCL-based fluxes (slope=0.50) as in most cases a non-linear model could not be fitted with only four data points. 48 % of the variance in QCL-based fluxes could be explained by fluxes from the GC method. Standard errors of the QCL method were again extremely low, i.e. <1 % of the

flux value and were always below 1.0 µg N m$^{-2}$ h$^{-1}$, while those from the GC method were on average in the range of 5 to 10 % of the flux value. Parallel operation of both methods was conducted from DOY 105 to 108. During this period, the campaign means were 117.8 ± 0.2 and 77.4 ± 8.2 µg N m$^{-2}$ h$^{-1}$ for the QCL and GC method, respectively.

As standard errors of QCL-based N$_2$O fluxes were on a constantly low level, no dependency on flux value was observed in any of the campaigns (Figure 7). The same was evident for GC-based fluxes in Braunschweig. At Risø, however, a slight but non-significant tendency of higher standard errors at higher flux rates was found. Only 8 % of GC data from Braunschweig met the criteria for flux calculation using the HMR model. At Risø, 38 % of GC data allowed for HMR flux calculation indicating that higher exchange regimes favor the usage of an exponential model when using the GC method. Similar findings (37 % allowance for non-linear model application) were reported by Petersen et al. (2011). Forbrich et al. (2010) found percentages of 13.6 %, 19.2 %, and 9.8 % of GC measurements on hummocks, lawns and flarks, respectively, which were best fitted with an exponential model. Their measurements, however, were made for methane fluxes and under an even larger $\partial c/\partial t$ range than was prevalent in our two campaigns. The fact that higher fluxes in our study were associated with lower standard errors and accepted HMR application corresponds well with $\kappa$ findings in Section 3.1 indicates that higher curvature in $c(t)$ coincided with higher fluxes.

In summary, our comparison of GC vs. QCL fluxes revealed that despite much higher precision, robustness, and temporal resolution in QCL measurements, GC is still a useful method to determine soil-atmosphere exchange of N$_2$O at longer time scales (here several weeks) when aiming at investigating N$_2$O budgets. Although single flux values particularly under low exchange regimes did not match well, campaign means were similar to those obtained by the QCL method. Under high exchange regimes, however, flux patterns matched considerably better, but resulted in larger absolute errors when comparing the campaign average, thereby leading to systematic errors (in our case an underestimation) when using the GC method at high N$_2$O fluxes for the assessment of N balances.

In general, chamber architecture is essential for headspace concentration buildup patterns given certain enclosure times, activity levels and headspace mixing. Our new chamber system performed well during the two campaigns for both analyzer setups. Through its specific design with not only vertically but also horizontally moving chambers, it will keep the soil column under relatively natural conditions. The only problem emerged at Risø when the guiding racks were slightly distorted under high wind speed conditions, i.e. when half-hourly means of wind speed were higher than 6 m s$^{-1}$. However, this problem could easily be fixed by tightening the guy wires that are attached to the aluminum rack. Commonly observed winter problems such as unnatural accumulation of snow inside the chamber and rime ice formation on the guiding racks and soil frame were not tested within this study, but will likely affect the ease of operation during harsh winter conditions.

### 3.4 N$_2$O uptake and diurnal variation

From an ecological point of view, QCL measurements offer a new opportunity for robust quantification of soil N$_2$O consumption. As N$_2$O uptake via denitrification exists in theory and could be shown under controlled lab conditions (e.g.,

Firestone and Davidson, 1989), it has been a major challenge to measure reliable fluxes in the field due to the fact that the magnitude of $N_2O$ uptake by soils is usually very low (Schlesinger, 2013), thereby problematic to be determined by GC measurements that are subjected to low signal to noise ratios (e.g., Brümmer et al., 2008).

In our study, neither at Risø nor during the Braunschweig campaign soil $N_2O$ uptake was observed when using QCL based
5 measurements. In only very few cases (n=5) $c'(t)$ were initially found to be negative, however, these data, which exhibited abnormally high standard errors, were discarded due to mechanical malfunctioning of the chamber system as a result of non-closure caused by distorted guiding racks through very high wind speeds at Risø (*cf.* Section 3.3).

Regarding GC-based data, 2 out of 37 fluxes in Risø were negative. Note that GC-based fluxes in Risø were only determined between DOY 105.5 and 108.5 when fluxes were elevated due to fertilizer application. In Braunschweig, however, nearly 25
10 %, i.e. 50 out of 201 flux rates from the GC setup were showing $N_2O$ uptake with only 3 of the 50 negative flux rates being significant ($p<0.05$, $p$-values not corrected for multiple testing), thus stressing the challenge of a robust determination of soil consumption of this important greenhouse gas when using the common vial-GC approach. Due to the fact that in this study no $N_2O$ soil uptake was found when using the much more reliable QCL setup, a further investigation of this topic on a variety of soil types under different land uses, plant communities, and climatic conditions is highly desired.

15 Besides investigating possible $N_2O$ soil uptake, the QCL methodology offers the opportunity to study diurnal variability of $N_2O$ fluxes. In a recent study by Shurpali et al. (2016) it has been pointed out that neglecting diurnal variations leads to uncertainties in terrestrial $N_2O$ emission estimates and should therefore be carefully taken into account when calculating nitrogen budgets. Similar to our study (Figure 8), they found reversed diurnal patterns under differing flux magnitudes. Intriguingly, when mean $N_2O$ fluxes were in a range between 12 and 35 $\mu g\ N\ m^{-2}\ h^{-1}$, in both this study (Risø low flux
20 regime) and Shurpali et al. (2016) highest fluxes were found during nighttime and lowest fluxes around midday. A contrasting diurnal pattern was observed when fluxes were lower than during the Risø campaign, i.e. in Braunschweig (7.2 to 8.7 $\mu g\ N\ m^{-2}\ h^{-1}$) or much higher due to fertilizer application as in Shurpali et al. (2016) (230 to 475 $\mu g\ N\ m^{-2}\ h^{-1}$). In the latter campaigns, mean $N_2O$ fluxes were highest at midday and lowest during nighttime, which corresponds to earlier findings (*e.g.*, Christensen, 1983; Du et al., 2006; Parkin and Kaspar, 2006; Brümmer et al., 2008; Alves et al., 2012) where
25 temperature was proved to be the main controlling factor for $N_2O$ soil-atmosphere exchange. Our study highlights that through its high time resolution QCL-based measurements will not only help enhance process understanding of $N_2O$ exchange by disentangling the strength of different drivers of $N_2O$ production like temperature, soil moisture, nitrogen availability, and microbial activity, but has also the potential to provide new insight into bidirectional exchange characteristics of other trace gases such as $CH_4$.

30

**Biogeosciences** Open Access
Discussions
EGU

**Acknowledgements**

**References**

Alves, B.J.R., Smith, K.A., Flores, R.A., Cardoso, A.S., Oliveira, W.R.D., Jantalia, C.P., Urquiaga, S., and Boddey, R.M.: Selection of the most suitable sampling time for static chambers for the estimation of daily mean $N_2O$ flux from soils. Soil Biol. Biochem. 46, 129−135, 2012.

Ammann, C., Wolff, V., Marx, O., Brümmer, C., and Neftel, A.: Measuring the biosphere-atmosphere exchange of total reactive nitrogen by eddy covariance. Biogeosciences 9, 4247−4261, 2012.

Anthony, W.H., Hutchinson, G.L., and Livingston, G.P.: Chamber measurement of soil–atmosphere gas exchange: Linear vs. diffusion-based flux models. Soil Sci. Soc. Am. J. 59, 1308−1310, 1995.

Baldocchi, D.D., Falge, E., Gu, L., Olson, R., Hollinger, D., Running, S., Anthoni, P., Bernhofer, C., Davis, K., Evans, R., Fuentes, J., Goldstein, A., Katul, G., Law, B.E., Lee, X., Malhi, Y., Meyers, T., Munger, W., Oechel, W., Paw U, K.T., Pilegaard, K., Schmid, H.P., Valentini, R., Verma, S., Vesala, T., Wilson, K., and Wofsy, S.C.: FLUXNET: A new tool to study the temporal and spatial variability of ecosystem-scale carbon dioxide, water vapor and energy flux densities. B. Am. Meteorol. Soc. 82, 2415−2434, 2001.

Brümmer, C., Brüggemann, N., Butterbach-Bahl, K., Falk, U., Szarzynski, J., Vielhauer, K., Wassmann, R., and Papen, H.: Soil-atmosphere exchange of $N_2O$ and NO in near-natural savanna and agricultural land in Burkina Faso (W. Africa). Ecosystems 11, 582−600, 2008.

Brümmer, C., Black, T.A., Jassal, R.S., Grant, N.J., Spittlehouse, D.L., Chen, B., Nesic, Z., Amiro, B.D., Arain, M.A., Barr, A.G., Bourque, C.P.A., Coursolle, C., Dunn, A.L., Flanagan, L.B., Humphreys, E.R., Lafleur, P.M., Margolis, H.A., McCaughey, J.H., and Wofsy, S.C.: How climate and vegetation type influence evapotranspiration and water use efficiency in Canadian forest, peatland and grassland ecosystems. Agric. For. Meteorol. 153, 14−30, 2012.

Brümmer, C., Marx, O., Kutsch, W.L., Ammann, C., Wolff, V., Fléchard, C.R., and Freibauer, A.: Fluxes of total reactive atmospheric nitrogen ($\sum N_r$) using eddy covariance above arable land. Tellus B 65, 19770, http://dx.doi.org/10.3402/tellusb.v65i0.19770, 2013.

Burnham, K.P. and Anderson, D.R.: Multimodel Inference: Understanding AIC and BIC in Model Selection, Sociol. Method. Res. 33, 261−304, 2004.

Butterbach-Bahl, K., Baggs, E.M., Dannenmann, M., Kiese, R., and Zechmeister-Boltenstern, S.: Nitrous oxide emissions from soils: how well do we understand the processes and their controls? Philos. T. Roy. Soc. B 368, doi: 10.1098/rstb.2013.0122, 2013.

Castaldi, S., de Grandcourt, A., Rasile, A., Skiba, U., and Valentini, R.: $CO_2$, $CH_4$ and $N_2O$ fluxes from soil of a burned grassland in Central Africa. Biogeosciences 7, 3459−3471, 2010.

Chapuis-Lardy, L., Wrage, N., Metay, A., Chotte, J.L., and Bernoux, M.: Soils, a sink for $N_2O$? A review. Glob. Change Biol. 13, 1−17, 2007.

Christiansen, J.R., Korhonen, J.F.J., Juszczak, R., Giebels, M., and Pihlatie, M.: Assessing the effects of chamber placement, manual sampling and headspace mixing on $CH_4$ fluxes in a laboratory experiment. Plant Soil 343, 171−185, 2011.

Christensen, S.: Nitrous oxide emission from a soil under permanent grass: Seasonal and diurnal fluctuations as influenced by manuring and fertilization. Soil Biol. Biochem. 15(5), 531−536, 1983.

Dannenmann, M., Gasche, R., Ledebuhr, A., Holst, T., Mayer, H., and Papen, H.: The effect of forest management on trace gas exchange at the pedosphere-atmosphere interface in beech (Fagus sylvatica L.) forests stocking on calcareous soils. Eur. J. Forest Res. 126, 331−346, 2007.

Denmead, O.T., MacDonald, B.C.T., Bryant, G., Naylor, T., Wilson, S., Griffith, D.W.T., Wang, W.J., Salter, B., White, I., and Moody, P.W.: Emissions of methane and nitrous oxide from Australian sugarcane soils. Agric. For. Meteorol. 150, 748−756, 2010.

Donoso, L., Santana, R., and Sanhueza, E.: Seasonal variation in $N_2O$ fluxes at a tropical savanna site: soil consumption of $N_2O$ during the dry season. Geophys. Res. Lett. 20, 1379−1382, 1993.

Du, R., Lu, D., and Wang, G.: Diurnal, seasonal, and inter-annual variations of $N_2O$ fluxes from native semi-arid grassland soils of Inner Mongolia. Soil Biol. Biochem. 38, 3474−3482, 2006.

Firestone, M.K. and Davidson, E.A.: Microbiological basis of NO and $N_2O$ production and consumption in soil. In: Andreae, M.O., Schimel, D.S., Eds. Exchange of trace gases between terrestrial ecosystems and the atmosphere. Chichester: John Wiley and Sons Ltd. pp 7−21, 1989.

Flessa, H. Ruser, R., Schilling, R., Loftield, N., Munch, J.C., Kaiser, E.A., and Beese, F.: $N_2O$ and $CH_4$ fluxes in potato fields: automated measurement, management effects and temporal variation. Geoderma 105, 307−325, 2002.

Forbrich, I., Kutzbach, L., Hormann, A., and Wilmking, M.: A comparison of linear and exponential regression for estimating diffusive $CH_4$ fluxes by closed-chambers in peatlands. Soil Biol. Biochem. 42, 507−515, 2010.

Horii, C.V., Munger, J.W., and Wofsy, S.C.: Fluxes of nitrogen oxides over a temperate deciduous forest. J. Geophys. Res. 109, D08305, doi:10.1029/2003JD004326, 2004.

Huber, P.J.: Robust Statistics. J. Wiley, New York, 1981.

Hutchinson, G.L. and Mosier, A.R.: Improved soil cover method for field measurement of nitrous oxide fluxes. Soil Sci. Soc. Am. J. 45, 311−316, 1981.

Hutchinson, G.L., Livingston, G.P., Healy, R.W., and Striegl., R.G.: Chamber measurement of surface−atmosphere trace gas exchange: Dependence on soil, interfacial layer, and source/sink properties. J. Geophys. Res. 105, 8865−8875, 2000.

IPCC: Climate Change 2013: The Physical Science Basis. Contribution of Working Group I to the Fifth Assessment Report of the Intergovernmental Panel on Climate Change. In: Stocker, T.F., D. Qin, G.-K. Plattner, M. Tignor, S.K. Allen, J. Boschung, A. Nauels, Y. Xia, V. Bex, and P.M. Midgley (eds.). Cambridge University Press, Cambridge, United Kingdom and New York, NY, USA, 2013.

Jassal, R.S., Black, T.A., Chen, B., Roy, R., Nesic, Z., Spittlehouse, D.L., and Trofymow, J.A.: $N_2O$ emissions and carbon sequestration in a nitrogen-fertilized Douglas fir stand. J. Geophys. Res. 113, G04013, DOI: 10.1029/2008JG000764, 2008.

Jassal, R.S., Black, T.A., Roy, R., and Ethier, G.: Effect of nitrogen fertilization on $CH_4$ and $N_2O$ fluxes, and bole and soil respiration. Geoderma 162, 182−186, 2011.

Jones, S.K., Famulari, D., Di Marco, C.F., Nemitz, E., Skiba, U.M., Rees, R.M., and Sutton, M.A.: Nitrous oxide emissions from managed grassland: a comparison of eddy covariance and static chamber measurements. Atmos. Meas. Tech. 4, 2179−2194, 2011.

Jury, W.A., Letey, J., and Collins, T.: Analysis of chamber methods used for measuring nitrous oxide production in the field. Soil Sci. Soc. Am. J. 46, 250−256, 1982.

Kroon, P.S., Hensen, A., van den Bulk, W.C.M., Jongejan, P.A.C., and Vermeulen, A.T.: The importance of reducing the systematic error due to non-linearity in $N_2O$ flux measurements by static chambers. Nutr. Cycl. Agroecosys. 82, 175−186, 2008.

Kroon, P.S., Schuitmaker, A., Jonker, H.J.J., Tummers, M.J., Hensen, A., and Bosveld, F.C.: An evaluation by laser Doppler anemometry of the correction algorithm based on Kaimal cospectra for high frequency losses of EC flux measurements of $CH_4$ and $N_2O$. Agric. For. Meteorol. 150, 794−805, 2010.

Kutsch, W.L., Aubinet, M., Buchmann, N., Smith, P., Osborne, B., Eugster, W., Wattenbach, M., Schrumpf, M., Schulze, E.D., Tomelleri, E., Ceschia, E., Bernhofer, C., Beziat, P., Carrara, A., Di Tommasi, P., Grünwald, T., Jones, M., Magliulo, V., Marloie, O., Moureaux, C., Olioso, A., Sanz, M.J., Saunders, M., Sogaard, H., and Ziegler, W.: The net biome production of full crop rotations in Europe. Agr. Ecosyst. Environ. 139, 336−345, 2010.

Kutzbach, L., Schneider, J., Sachs, T., Giebels, M., Nykänen, H., Shurpali, N. J., Martikainen, P. J., Alm, J., and Wilmking, M.: $CO_2$ flux determination by closed-chamber methods can be seriously biased by inappropriate application of linear regression. Biogeosciences 4, 1005−1025, 2007.

Leiber-Sauheitl, K., Fuß, R., Voigt, C., and Freibauer, A.: High $CO_2$ fluxes from grassland on histic Gleysol along soil carbon and drainage gradients. Biogeosciences 11, 749−761, 2014.

Livesley, S.J., Grover, S., Hutley, L.B., Jamali, H., Butterbach-Bahl, K., Fest, B., Beringer, J., and Arndt, S.: Seasonal variation and fire effects on $CH_4$, $N_2O$ and $CO_2$ exchange in savanna soils of northern Australia. Agric. For. Meteorol. 151, 1440−1452, 2011.

Livingston, G.P., Hutchinson, G.L., and Spartalian, K.: Trace gas emission in chambers: a non-steady-state diffusion model. Soil Sci. Soc. Am. J. 70, 1459−1469, 2006.

Loftfield, N., Flessa, H., Augustin, J., and Beese, F.: Automated gas chromatographic system for rapid analysis of the trace gases methane, carbon dioxide, and nitrous oxide. J. Environ. Qual. 26, 560−564, 1997.

Lohila, A., Aurela, M., Hatakka, J., Pihlatie, M., Minkkinen, K., Penttil, T., and Laurila, T.: Responses of $N_2O$ fluxes to temperature, water table and N deposition in a northern boreal fen. Eur. J. Soil Sci. 61, 651−661, 2010.

Matthias, A.D., Yarger, D.N., and Weinbeck, R.S.: A numerical evaluation of chamber methods for determining gas fluxes. Geophys. Res. Lett. 5, 765−768, 1978.

Merbold, L., Eugster, W., Stieger, J., Zahniser, M., Nelson, D. D., and Buchmann, N.: Greenhouse gas budget ($CO_2$, $CH_4$ and $N_2O$) of intensively managed grassland following restoration. Glob. Change Biol. 20, 1913−1928, 2014.

Moffat, A.M.: A new methodology to interpret high resolution measurements of net carbon fluxes between terrestrial ecosystems and the atmosphere. Doctoral Thesis, Department of Mathematics and Computer Science, Friedrich Schiller University, Jena, 2012.

Neftel, A., Ammann, C., Fischer, C., Spirig, C., Conen, F., Emmenegger, L., Tuzson, B., and Wahlen, S.: $N_2O$ exchange over managed grassland: Application of a quantum cascade laser spectrometer for micrometeorological flux measurements. Agric. For. Meteorol. 150, 775−785, 2010.

Nakano, T., Sawamoto, T., Morishita, T., Inoue, G., and Hatano, R.: A comparison of regression methods for estimating soil−atmosphere diffusion gas fluxes by a closed-chamber technique. Soil Biol. Biochem. 36, 107−113, 2004.

Nelson, D.D., McManus, B., Urbanski, S., Herndon, S., and Zahniser, M.S.: High precision measurements of atmospheric nitrous oxide and methane using thermoelectrically cooled mid-infrared quantum cascade lasers and detectors. Spectrochim. Acta A 60, 3325−3335, 2004.

Papen, H. and Butterbach-Bahl, K.: A 3-year continuous record of nitrogen trace gas fluxes from untreated and limed soil of a N-saturated spruce and beech forest ecosystem in Germany, 1. $N_2O$ emissions. J. Geophys. Res. 104, 18487−18503, 1999.

Parkin, T.B. and Kaspar, T.C.: Nitrous Oxide Emissions from Corn–Soybean Systems in the Midwest. J. Environ. Qual. 35, 1496−1506, 2006.

Parkin, T.B. and Venterea, R.T.: Chamber-based trace gas flux measurements. USDA-ARS GRACEnet Project Protocols Chapter 3. Web access: http://www.ars.usda.gov/SP2UserFiles/Program/212/Chapter%203.%20GRACEnet%20Trace%20Gas%20Samplin g%20Protocols.pdf, 2010.

Pedersen, A.R., Petersen, S.O., and Schelde, K.: A comprehensive approach to soil-atmosphere trace-gas flux estimation with static chambers. Eur. J. Soil Sci. 61, 888−902, 2010.

Petersen, S.O., Mutegi, J.K., Hansen, E.M., and Munkholm, L.J.: Tillage effects on $N_2O$ emissions as influenced by a winter cover crop. Soil Biol. Biochem. 43, 1509−1517, 2011.

Pihlatie, M.K., Christiansen, J.R., Aaltonen, H., Korhonen, J.F., Nordbo, A., Rasilo, T., Benanti, G., Giebels, M., Helmy, M., Sheehy, J., Jones, S., Juszczak, R., Klefoth, R., Lobo-do-Vale, R., Rosa, A.P., Schreiber, P., Serca, D., Vicca, S., Wolf, B., and Pumpanen, J.: Comparison of static chambers to measure $CH_4$ emissions from soils. Agric. For. Meteorol. 171, 124−136, 2013.

R Core Team: R: A language and environment for statistical computing, available at: http://www.R-project.org/, 2012.

Rinne, J., Pihlatie, M., Lohila, A., Thum, T., Aurela, M., Tuovinen, J., Laurila, T., and Vesala, T.: Nitrous oxide emissions from a municipal landfill. Environ. Sci. Technol. 39, 7790−7793, 2005.

Rolston, D.E.: Gas diffusivity. In A. Klute (ed.) Methods of soil analysis. Part 1. Physical and mineralogical methods. Agron. Monogr. 9., p. 1089−1102. 2nd ed. ASA and SSSA, Madison, WI, 1986.

Rosenkranz, P., Brüggemann, N., Papen, H., Xu, Z., Horváth, L., and Butterbach-Bahl, K.: Soil N and C trace gas fluxes and microbial soil N turnover in a sessile oak (Quercus petraea (Matt.) Liebl.) forest in Hungary. Plant Soil 286, 301−22, 2006.

Rothman, L.S., Gordon, I.E., Barbe, A., Benner, D.C., Bernath, P.F., Birk, M., Boudon, V., Brown, L.R., Campargue, A., Champion, J.-P., Chance, K., Coudert, L.H., Dana, V., Devi, V.M., Fally, S., Flaud, J.-M., Gamache, R.R., Goldman, A., Jacquemart, D., Kleiner, I., Lacome, N., Lafferty, W., Mandin, J.-Y., Massie, S.T., Mikhailenko, S.N., Miller, C.E., Moazzen-Ahmadi, N., Naumenko, O.V., Nikitin, A.V., Orphal, J., Perevalov, V.I., Perrin, A., Predoi-Cross, A., Rinsland, C.P., Rotger, M., Simeckova, M., Smith, M.A.H., Sung, K., Tashkun, S.A., Tennyson, J., Toth, R.A., Vandaele, A.C., and Vander Auwera J.: The HITRAN 2008 molecular spectroscopic database. J. Quant. Spectrosc. Ra. 110, 533−572, 2009.

Savage, K., Phillips, R., and Davidson, E.: High temporal frequency measurements of greenhouse gas emissions from soils. Biogeosciences 11, 2709−2720, 2014.

Schiller, C.L. and Hastie, D.R.: Nitrous oxide and methane fluxes from perturbed and unperturbed boreal forest sites in northern Ontario. J. Geophys. Res. 101, 22,767− 22,774, 1996.

16

Schlesinger, W. H.: An estimate of the global sink for nitrous oxide in soils. Glob. Change Biol. 19(10), 2929−2931, 2013.

Seinfeld, J.H. and Pandis, S.N.: Atmospheric Chemistry and Physics – From Air Pollution to Climate Change. $2^{nd}$ ed. John Wiley & Sons, Inc., Hoboken, New Jersey, 1232 pp, 2006.

Shurpali, N.J., Rannik, Ü., Jokinen, S., Lind, S., Biasi, C., Mammarella, I., Peltola, O., Pihlatie, M., Hyvönen, N., Räty, M.,
Haapanala, S., Zahniser, M., Virkajärvi, P., Vesala, T., and Martikainen, P.J.: Neglecting diurnal variations leads to uncertainties in terrestrial nitrous oxide emissions. Scientific Reports 6:25739, DOI: 10.1038/srep25739, 2016.

Thomson, A.J., Giannopoulos, G., Pretty, J., Baggs, E.M., and Richardson, D.J.: Biological sources and sinks of nitrous oxide and strategies to mitigate emissions. Philos. T. Roy. Soc. B 367, 1157−1168, 2012.

Tuzson, B., Hiller, R.V., Zeyer, K., Eugster, W., Neftel, A., Ammann, C., and Emmenegger, L.: Field intercomparison of two optical analyzers for $CH_4$ eddy covariance flux measurements. Atmos. Meas. Tech. 3, 1519−1531, 2010.

Wrage, N., Velthof, G.L., van Beusichem, M.L., and Oenema, O.: Role of nitrifier denitrification in the production of nitrous oxide. Soil Biol. Biochem. 33(12), 1723−1732, 2001.

**Table 1. Supplementary information on field campaigns.**

|  | **Braunschweig** | **Risø** |
|---|---|---|
| **Coordinates** | 52°17'52''N, 10°26'36''O | 55°40'50''N, 12°06'05''O |
| **Start observation period** | Nov 13, 2012 | Apr 10, 2013 |
| **End observation period** | Dec 12, 2012 | Apr 24, 2013 |
| **Total GC flux rates (n)** | 201 | 37 |
| **Total QCL flux rates (n)** | 187 | 158 |
| **Land use** | Grassland | Willow field (harvested) |
| **Fertilization, date** | No fertilization | Apr 9, 2013 |
| **Fertilization, amount** | No fertilization | 120 kg N ha$^{-1}$ |
| **Fertilization, type** | No fertilization | Mineral (ammonium nitrate), N-P-K 21-3-10 |
| **Soil texture** | Silty sand | Sandy loam |
| **Soil type** | Cambisol | Luvisol |
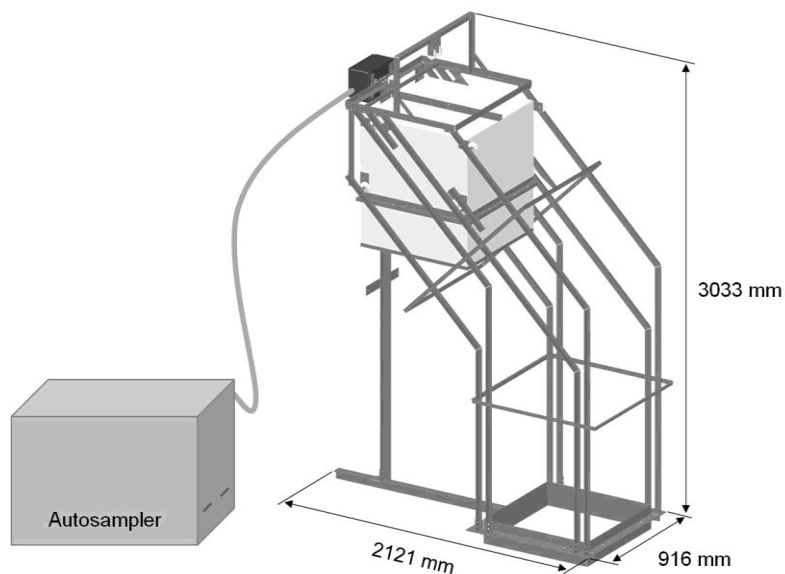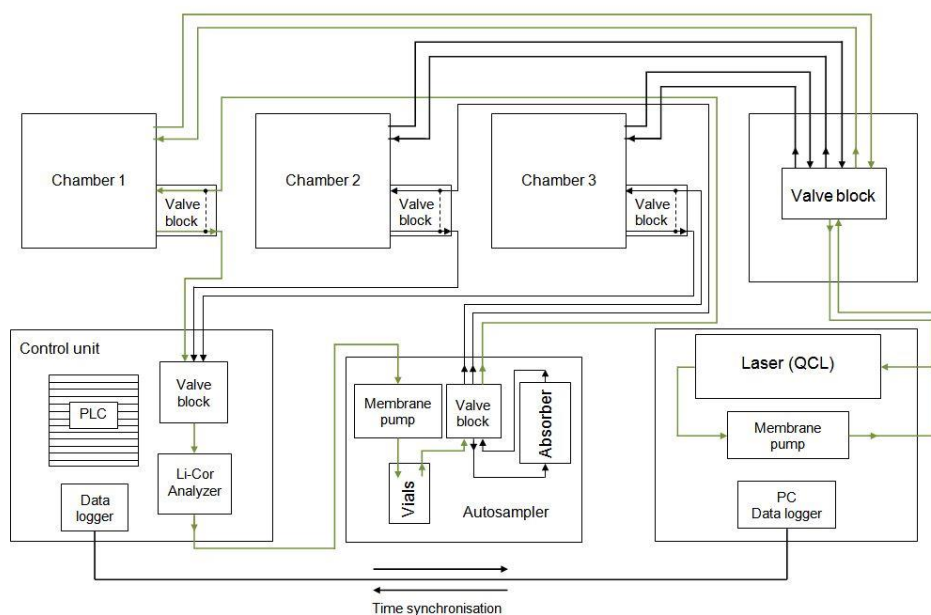
**Figure 1. Schematic diagrams of an automated chamber connected to an autosampler unit (A) and of the entire chamber system (B). Green lines indicate that Chamber 1 is currently in measurement mode. See text for detailed description.**
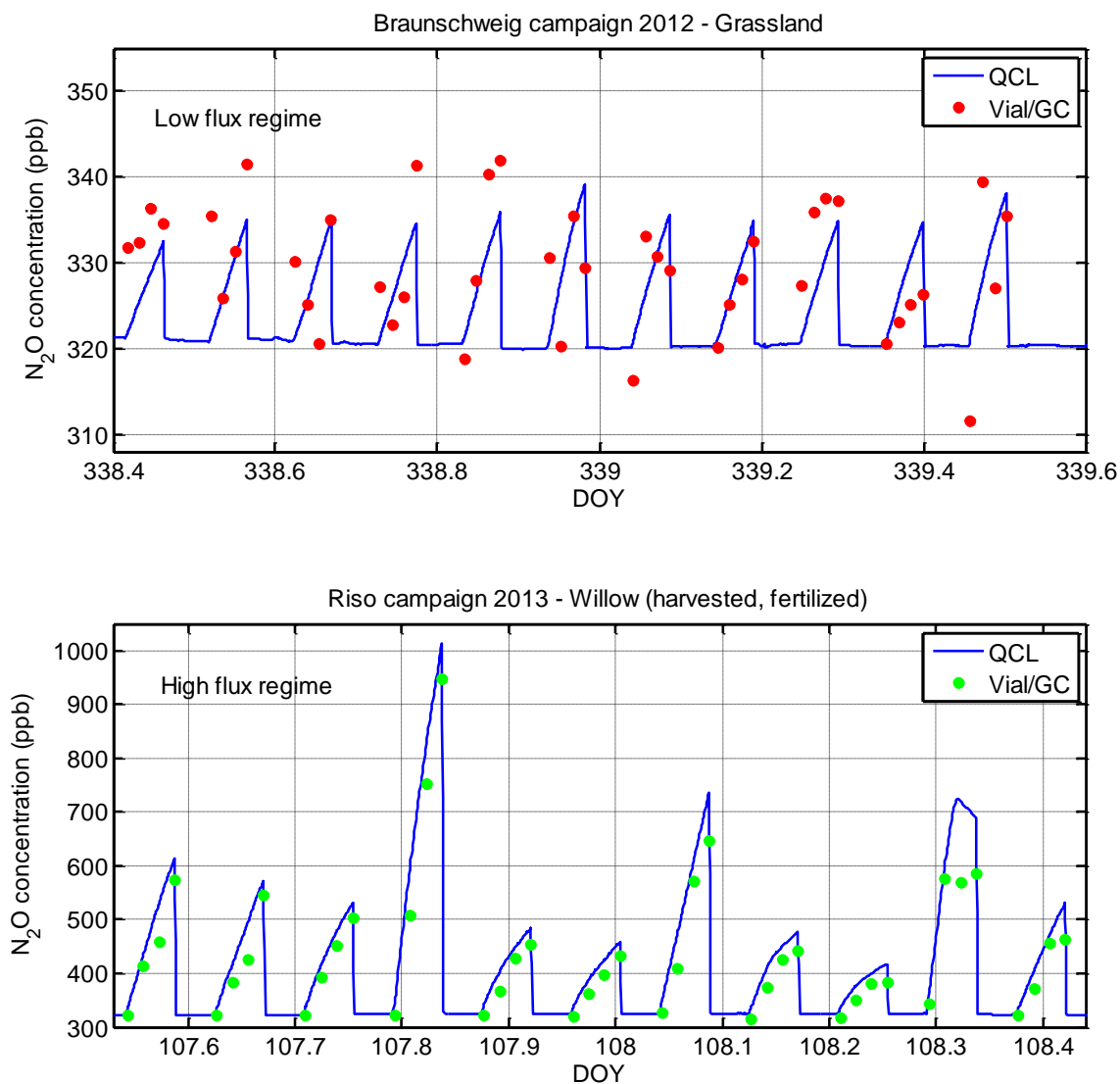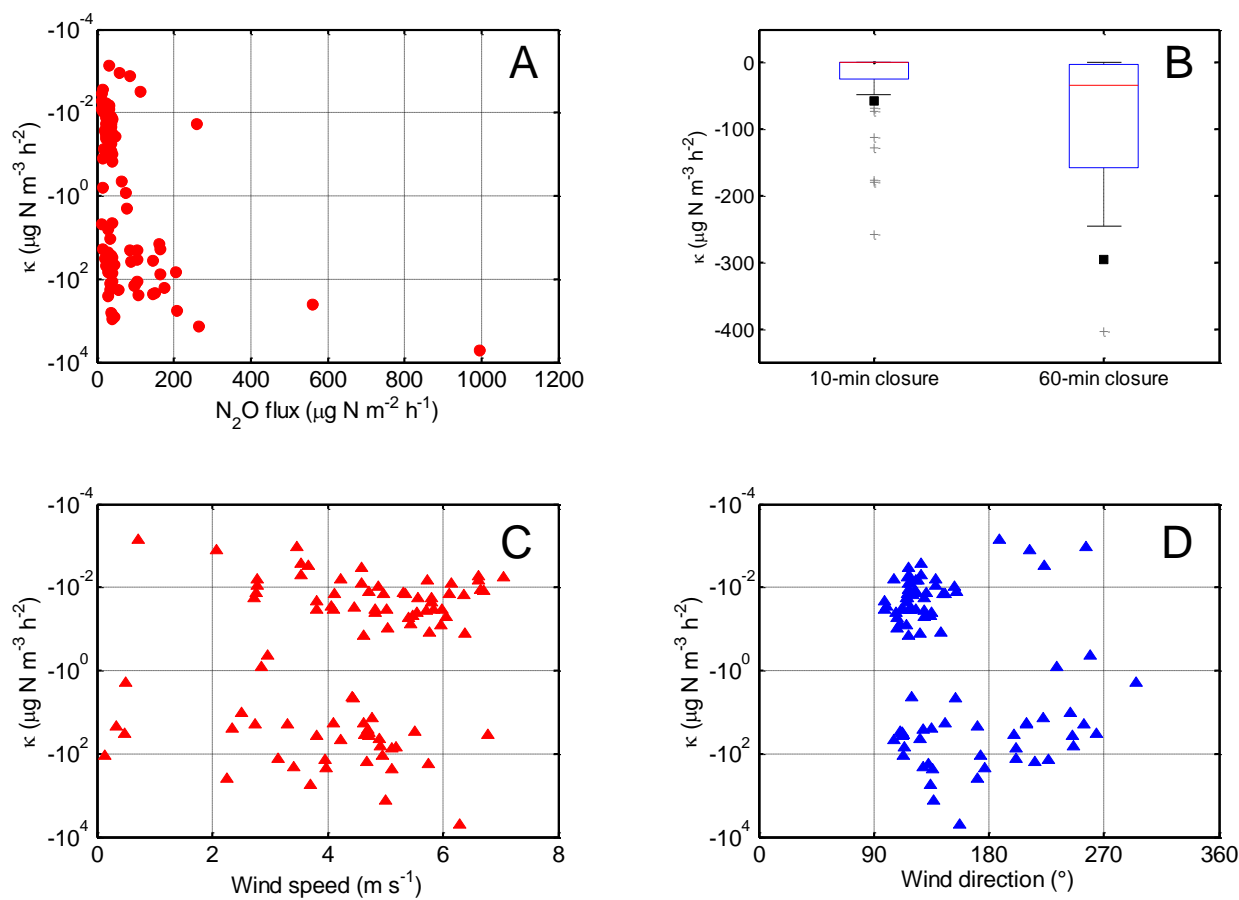
**Figure 2.** Examples of time series of $N_2O$ chamber concentrations during the Braunschweig (upper panel) and Risø campaign (lower panel). Chambers were periodically closed for 60 minutes. Vials were filled with sample air at $t_0$, $t_{20}$, $t_{40}$, and $t_{60}$. The QCL system was operated at a sampling frequency of 10 Hz; plotted are 1-min means.

**Figure 3. Panels A: Relationship between** $\kappa$ **and N$_2$O fluxes calculated with an exponential model (see text for details). The parameter** $\kappa$ **indicates the curvature, i.e. the second derivative of the exponential model used for flux calculation. Negative** $\kappa$ **values correspond to concave functions, i.e. plateauing (saturating) N$_2$O concentration increases (*cf*. Figure 2). Panel B: Box plot of** $\kappa$ **values showing the difference between 10 and 60-min closure where black squares represent the arithmetic mean, red horizontal lines indicate the median, blue horizontal lines indicate lower and upper quartile values, black whiskers represent the interquartile range and outliers from this range are plotted as grey crosses. To ensure better readability, the y-axis is truncated at −450 µg N m$^{-3}$ h$^{-2}$. Thus, some outliers between −450 and −10$^4$ µg N m$^{-3}$ h$^{-2}$ are not shown. Panel C and D: Relationship between** $\kappa$ **and wind speed (C) as well as** $\kappa$ **and wind direction (D). All data are taken from the quantum cascade laser system operated during the Risø campaign. Chambers were closed for 10 minutes at DOY <105.5 and for 60 minutes at DOY >105.5.**
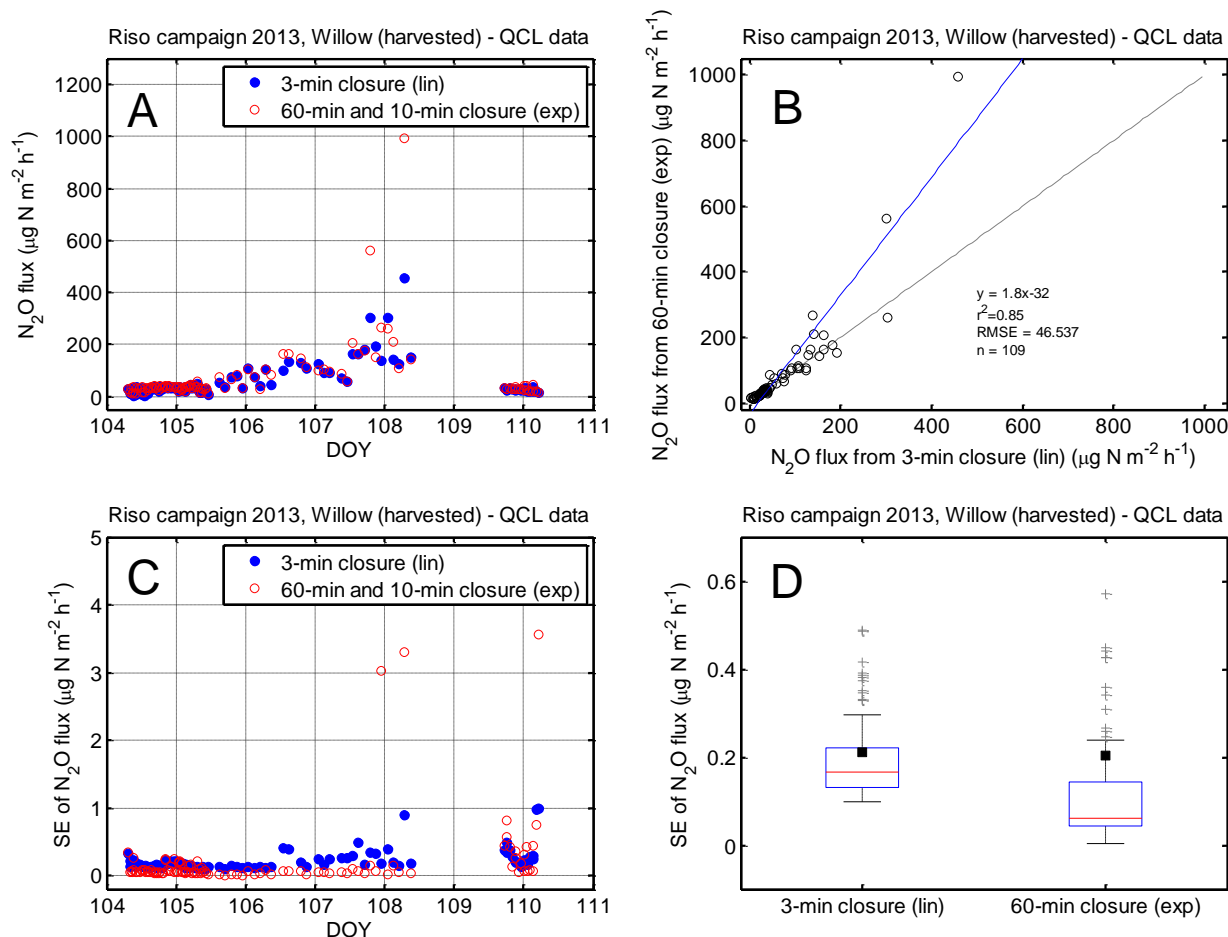
**Figure 4. Comparison of N$_2$O fluxes measured during the Risø campaign by the QCL system based on different calculation methods, i.e. a linear model using only the first three minutes of data after chamber closure (filled blue circles) and an exponential model (open red circles) (see text) using either the full 60 minutes (DOY 105.5 to DOY 108.5) or the full 10 minutes of data (DOY <105.5 and DOY >108.5) (Panel A) with associated standard errors (SE) of N$_2$O fluxes (Panel C). Also shown is a linear regression analysis (orthogonal) of N$_2$O fluxes calculated by the exponential model (60 and 10 minutes of data) vs. N$_2$O fluxes calculated by the linear model (3 minutes of data) (Panel B) and a box plot of associated standard errors of N$_2$O fluxes (Panel D) showing the difference between 3 and 60-min closure. Black squares represent the arithmetic mean, red horizontal lines indicate the median, blue horizontal lines indicate lower and upper quartile values, black whiskers represent the interquartile range and outliers from this range are plotted as grey crosses. To ensure better readability, the y-axis is truncated at +0.7 µg N m$^{-2}$ h$^{-1}$. Thus, few outliers between 0.7 and 4 µg N m$^{-2}$ h$^{-1}$ are not shown.**
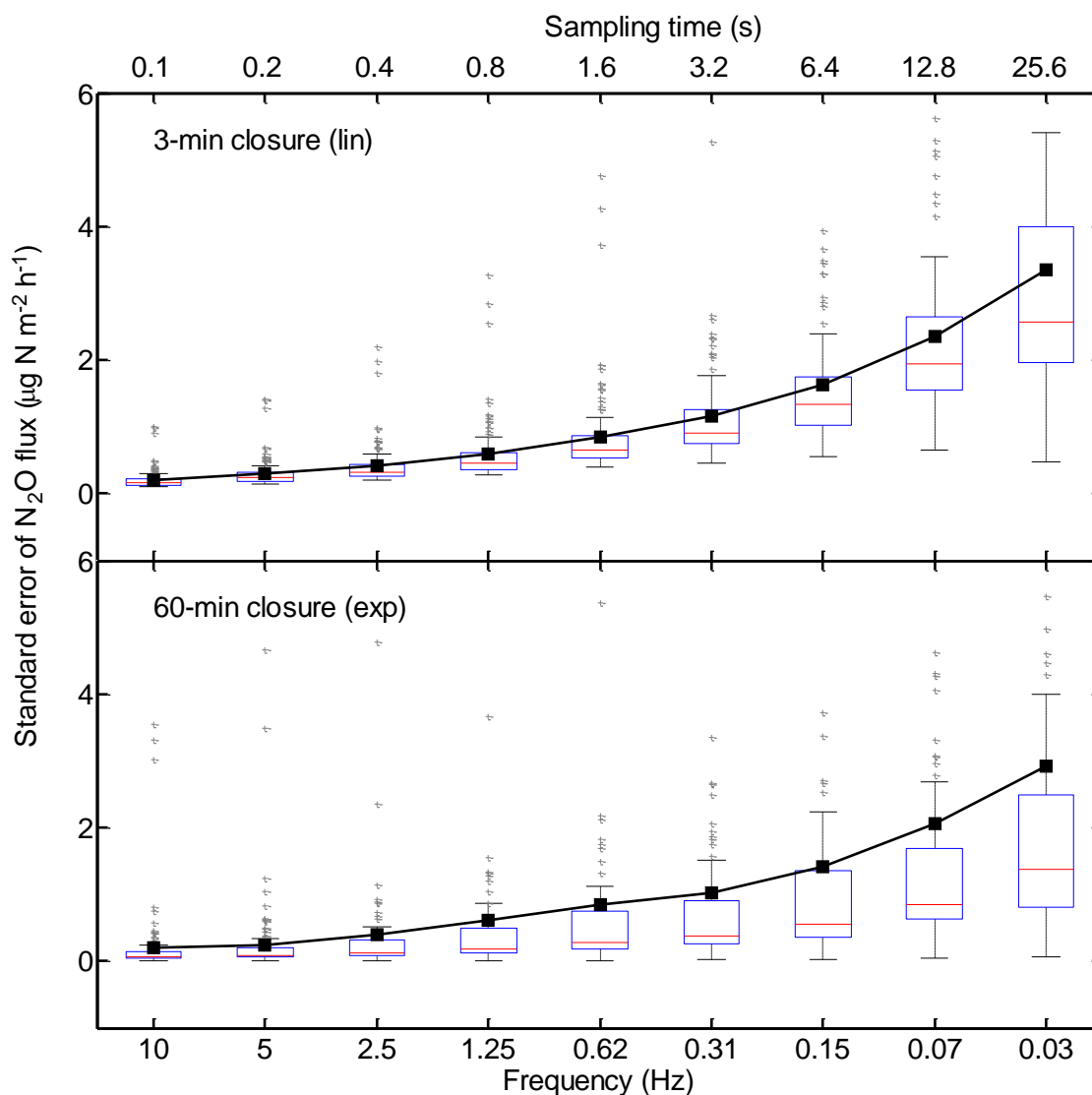
**Figure 5. Dependency of standard errors of N₂O fluxes on measurement frequency when using only the first 3 minutes of data
after chamber closure (linear model; upper panel) and the full 60-minute dataset (exponential model; lower panel). Black squares
represent the arithmetic mean, red horizontal lines indicate the median, blue horizontal lines indicate lower and upper quartile
values, black whiskers represent the interquartile range and outliers from this range are plotted as grey crosses. For better
readability, the y-axis is truncated at +6 µg N m$^{-2}$ h$^{-1}$. Thus, few outliers are not shown.**
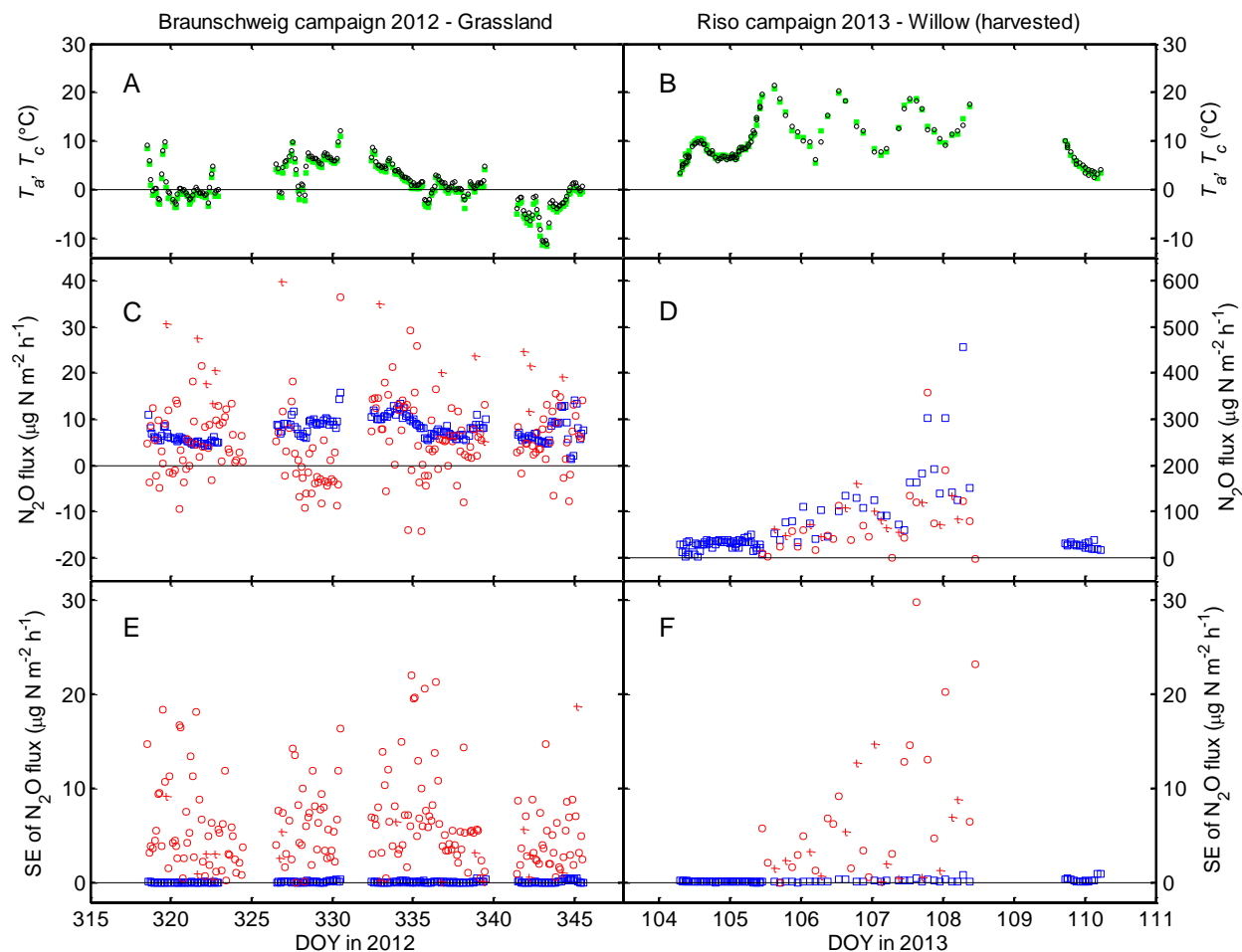
Figure 6. Time series of air ($T_a$, green markers) and chamber temperatures ($T_c$, black markers)(panels A and B), N$_2$O fluxes and the respective standard errors of N$_2$O fluxes during the Braunschweig (panels C and E) and the Risø campaign (panels D and F). Blue markers indicate QCL data, red markers indicate GC data. Crosses are plotted for GC data when all criteria for flux calculation using the exponential HMR model were met (see text for details), otherwise circles are plotted indicating the usage of a linear model for flux calculation.
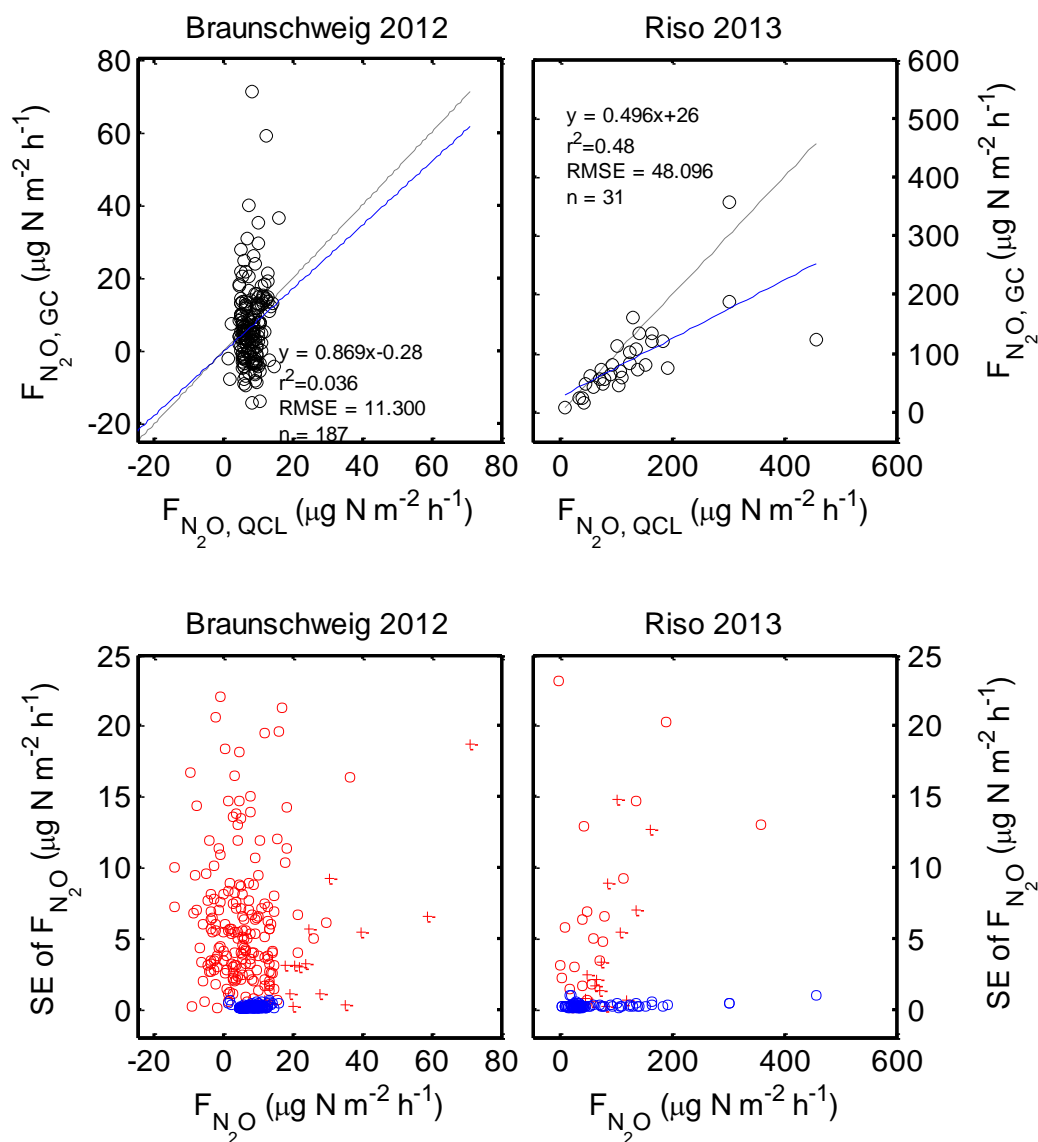
**Figure 7. GC vs. QCL-based N$_2$O fluxes (upper panels) and relationships between standard errors (SE) of N$_2$O fluxes and the respective flux values (lower panels) during the Braunschweig (panels on left-hand side) and the Risø campaign (panels on the right-hand side). Blue markers indicate QCL data, red markers indicate GC data. Crosses are plotted for GC data when all criteria for flux calculation using the exponential HMR model were met (see text for details), otherwise circles are plotted indicating the usage of a linear model for flux calculation.**
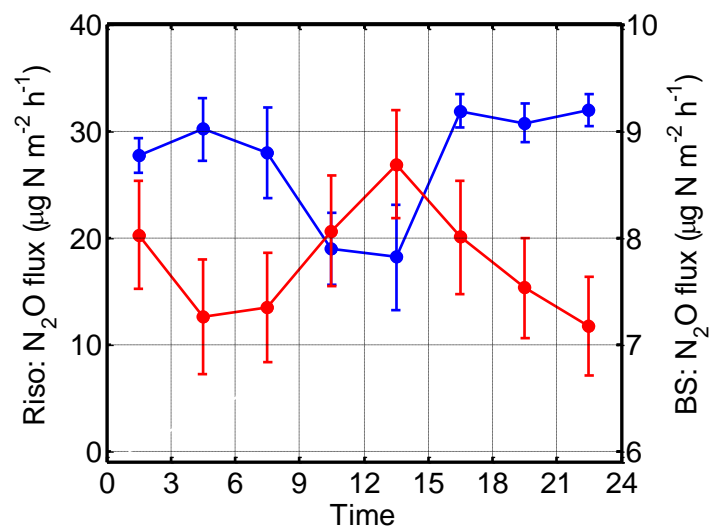
**Figure 8. Mean diurnal courses of N$_2$O fluxes derived from QCL flux measurements during the Risø (blue line) and Braunschweig**
5 **(red line) campaign. To exclude fertilization effects in Risø, only data from the low flux period (DOY<105.5 and >108.5) were**
**taken.**